Circulation effects on nitrogen dynamics in the Ionian Sea

Ionian Sea
Nitrogen cycle
General circulation
Ecomodel
Primary production

Mer Ionienne
Cycle de l'azote
Circulation générale
Modèle écologique
Production primaire

Giuseppe CIVITARESE [a], Alessandro CRISE [b], Guido CRISPI [b] and Renzo MOSETTI [b]

[a] Istituto Talassografico di Trieste CNR, Viale Romolo Gessi 2, 34100 Trieste, Italy.

[b] Osservatorio Geofisico Sperimentale, P.O. Box 2011, 34016 Trieste, Italy.

Received 06/04/95, in revised form 29/12/95, accepted 09/01/96.

ABSTRACT

In this work the description of the interaction between the general circulation and the nitrogen cycle in the Ionian Sea is considered. Firstly, an analysis is made of nitrate data collected during POEM-BC cruises in October 1991 and April 1992; then a numerical experiment based on a coupled hydrodynamic ecomodel is presented. The model results relative to the periods corresponding to the cruises are discussed.

The ecomodel is climatological and represents an aggregated description of the nitrogen cycle in terms of inorganic nitrogen, phytoplankton and detritus. The numerical results as nitrogen distributions, fluxes and primary production are presented.

A strong dependence of nitrogen distribution on circulation emerges both from the observational data and from model simulations giving similar results in the upwelling areas and in the opposite effects of cyclonic and anticyclonic gyres. On a smaller scale, the experimental data present a more energetic structure than that obtained by the climatological model, suggesting the need for future development.

RÉSUMÉ

Effets de la circulation sur la dynamique de l'azote en Mer Ionienne.

Le présent travail décrit l'interaction entre la circulation générale et le cycle de l'azote dans la Mer Ionienne. Les données du nitrate ont été acquises au cours des campagnes POEM-BC en octobre 1991 et avril 1992, puis une expérience numérique a été effectuée à l'aide d'un modèle couplé, écologique et hydrodynamique.

Le modèle écologique est climatologique et il décrit le cycle de l'azote en termes d'azote inorganique, de phytoplancton et de détritus. Les résultats numériques sont présentés sous forme de répartitions d'azote, de flux et de production primaire.

Les données d'observation et la modélisation donnent des résultats analogues : une forte corrélation entre la répartition de l'azote et la circulation, dans les zones d'upwelling et dans les tourbillons cycloniques et anticycloniques. A plus petite échelle, les données expérimentales indiquent une structure plus énergétique que celle obtenue par le modèle climatologique, ce qui suggère la nécessité de travaux plus approfondis.

Oceanologica Acta, 1996, **19**, 6, 609-622.

INTRODUCTION

It is widely accepted that hydrodynamics strongly affects the biogeochemical cycles ultimately acting as a source of energy for the biomass (Margaleff, 1978), but the nature of the interaction between biological, chemical and physical processes is complex and far from fully understood.

The Eastern Mediterranean Sea is considered to be among the most oligotrophic areas in the world ocean. Its oligotrophy can be explained in terms of the inverse estuarine circulation induced by thermohaline processes. Primary production is in general very low, except in some coastal areas subjected to the influence of major rivers or to considerable anthropic pressure (Cruzado, 1994).

In this scenario, the Ionian Sea plays a crucial role as a basin connecting the Western and Levantine basins. The Western Mediterranean communicates with the Ionian Sea through the Sicily Strait, while the Otranto Strait separates the Adriatic from the Ionian Sea. At the eastern boundary, the Cretan Passage connects the Levantine basin with the Ionian.

In the latter basin, nutrient distributions and their seasonal dynamics are almost unknown because of a lack of systematic chemical and biological observations.

Vertical advection of nitrate provides the major source of new nitrogen, and thus new production (Dugdale and Goering, 1967). Also, in the Ionian Sea the exchange with deep waters is supposed to be the main process that relatively enriches the euphotic zone with the subsequent reduction of the nutrient concentration in the ocean interiors.

The effect of wind-induced mixing should be particularly pronounced during winter. After formation of the seasonal thermocline, biological production is principally fed by regenerated nitrogen. The prevalent anticyclonic circulation prevents any exchange from the deeper layers to the euphotic zone. In addition, the contributions in terms of dissolved and particulate organic nitrogen coming from the Sicily Strait should be considered in order to estimate the nitrogen budgets more correctly.

The exchanges between the Ionian Sea and the adjacent basins are strictly related to the new view of the dynamics and the biogeochemical budgets which is emerging after recent results mainly by the POEM Group. In particular, the analysis of the pooled hydrographic data collected during 1985-1987 cruises permits the following conclusions:

1) the Modified Atlantic Water (MAW) stream is permanent and is connected to the Mid-Mediterranean Jet (Golnaraghi and Robinson, 1994);

2) the inflow at the Sicily Strait constitutes the most important forcing for the Ionian circulation (Malanotte-Rizzoli and Bergamasco, 1991);

3) the superficial current in the Ionian Sea is weakly anticyclonic during summer, but does not constitute a permanent feature (POEM Group, 1992);

4) the large-scale gradients of temperature and salinity present in the basin have the same sign, making an opposite contribution to the state equation; no direct baroclinic large-scale circulation is therefore expected, at least in the summer regime (Nittis *et al.*, 1993);

5) the Ionian and Levantine basins are recognized to form one deep thermohaline cell; the turnover time of Eastern Mediterranean Deep Water (EMDW) is about 126 years (Roether and Schlitzer, 1991).

This work investigates the seasonal variability of the nutrient concentration in an oligotrophic basin such the Ionian Sea. In particular, the effects of both horizontal and vertical advection and diffusion will be studied, using a three-dimensional coupled hydrodynamic ecomodel.

In the following section, concerning Observational Data, the evidence emerging from the data collected during the POEM-BC cruises is discussed.

Next, in the Coupled Ecomodel section, we shall describe the model and its parameterization. The results of the numerical experiment are discussed in terms of horizontal and vertical behaviour of the tracers, of nitrogen fluxes and of total, regenerated and new production.

Finally, in the Discussion section, a verification of the model results with the experimental data is attempted. The Conclusion section sets out the future perspectives.

OBSERVATIONAL DATA

Within the frame of POEM-BC programme for the study of chemical and biological interactions with the physical aspects of the Eastern Mediterranean Basin, two interdisciplinary cruises (POEM-BC-O91 and POEM-BC-A92) were carried out in the Ionian Sea and Sicily Strait during October 1991 and April-May 1992. These cruises made it possible for the first time to investigate with a good resolution the horizontal and vertical distribution of dissolved oxygen and nutrients (nitrate, phosphate and silicate). In this section we illustrate some significative features of nitrate distribution in the Ionian Sea in October 1991 and April 1992.

Nitrate analyses were carried out on frozen samples (POEM-BC-O91) or immediately after collection on board (POEM-BC-A92) by means of a Chemlab autoanalyser according to the statements of the POEM Workshop on Bio-Chemical Intercalibration (Trieste, May 27-June 1, 1991).

The sampling grids for the two cruises are reported in Figure 1.

The horizontal distributions at 100 m and 300 m (Fig. 2) illustrate the situation of the basin approximately at the base and below the euphotic zone, respectively.

In October (Fig. 2 *a*), the whole area at a depth of 100 m is almost completely depleted, with nitrate values less than 0.5 μM except in the proximity of the Otranto Strait (Adriatic surface inflow) and in correspondence to the northwestern boundary of the basin.

In April (Fig. 2 *b*), the concentrations are higher. In the zones affected by small but relatively strong cyclonic gyres, nitrate concentrations assume values greater than 2 μM.

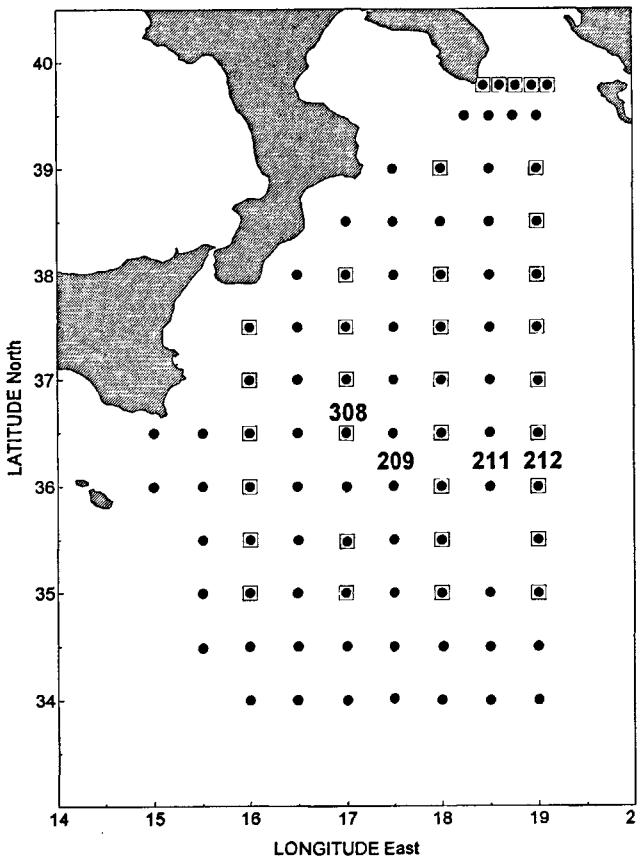

Figure 1

POEM-BC station grid: ⊡ POEM-BC-091 and POEM-BC-A92 common stations; • only POEM-BC-A92 stations.

At 300 m, the effect of the dynamics is particularly evident. In October (Fig. 2 *c*), a large anticyclonic gyre at the centre of the investigated area downwells, the water decreasing the nitrate content to values less than 2.5 μM. At the border of the gyre the concentrations increase to 5 μM.

In April (Fig. 2 *d*), the situation seems to be more energetic and shows a more complex behaviour: the concentrations are generally higher, especially in the upwelling area centred approximately at 36° N and 17.5° E.

The above considerations with regard to the effects of the circulation on nitrate distributions are consistent with the geopotential anomaly maps calculated from the CTD data of the two cruises (Michelato *et al.*, 1992; Kovacevic *et al.*, 1994).

In October 1991 (Fig. 3 *a*), a strong anticyclonic circulation dominates the whole basin and the centre of the anticyclonic area corresponds to the minimum of nitrate in Figure 2 *c*, while no signal is obviously present at 100 m depth (Fig. 2 *a*) because of the deepening of the nutrient-depleted layer below this depth.

In April (Fig. 3 *b*), the anticyclonic regime is modified by the presence of an intense cyclonic area in the southern part of the Ionian Sea, which is the main cause of the nitrate dome found at the same positions in Figure 2 *b* and Figure 2 *d*. This is surrounded by a number of anticyclonic eddies giving place to local nitrate minima in the same positions. Thus the circulation induced at the bottom of the euphotic zone (100 m) shows a seasonal reversal (cyclonic in winter – anticyclonic in summer), whereas at 300 m the dynamics seems to be much more complex.

Generally, the vertical distribution of nitrate in the Ionian Sea (Fig. 4) exhibits a first homogeneous layer (50-200 m thick depending on the season and the location), characterized by very low nitrate content, often very close to zero.

At the nitracline, the concentration gradually increases to its maximum value of 5.5-6.0 μM, in correspondence to the minimum value of dissolved oxygen. The deeper layers show a general decrease of concentration (less than 5 μM at the bottom).

The vertical profiles of nitrate of selected stations are reported in Figure 5, where the effects of the two seasonal circulation regimes are evidenced.

Generally, the depleted layer is thicker in October than in April, but the vertical positions and extensions of the nitracline follow the different circulation regimes in the two seasons.

An important feature emerging from the comparison of the two seasonal situations is the remarkable presence in April of advected new nitrogen in the euphotic layer. The seasonal pycnocline is gradually strengthening, but the cyclonic circulation pushes relatively nutrient-rich waters in the productive layer. In the Ionian Sea production probably follows an annual cycle, the primary production maximum occurring at the end of winter. While the situation in October is representative of the final stage of production (Rabitti *et al.*, 1994 *a*), the biological production in April is still active and fed by new nitrogen.

THE COUPLED ECOMODEL

The influence of the circulation on the nitrogen cycling in the Ionian Sea is studied through a tight coupling between the general circulation model (GCM) adapted to the entire Mediterranean Sea by Pinardi and Navarra (1993) and the aggregate ecological model (AEM) by Crise *et al.* (1992).

The GCM, forced by monthly mean Hellermann and Rosenstein winds, gives the evolution of the velocity, temperature and salinity. The surface of the basin is constrained to the Levitus climatological thermohaline fields.

This model is discretized through the Bryan (1967) and Cox (1984) finite differences numerical scheme on a horizontal grid of 1/4 degree size and on 16 vertical levels.

The domain of integration is the entire Mediterranean basin with realistic topography, avoiding the fictitious impositions at the open boundaries. The time-step of the simulations reported in this work is 1800 s. The topography of the Ionian Sea used in the model is shown in Figure 6.

The seasonal variation of the sub-basin scale gyres are determined by the forcing cycle in the wind-stress curl centres. The wind-induced circulation reverses the gyre present in the centre of the Ionian Sea from cyclonic during the winter to weakly anticyclonic in the summer.

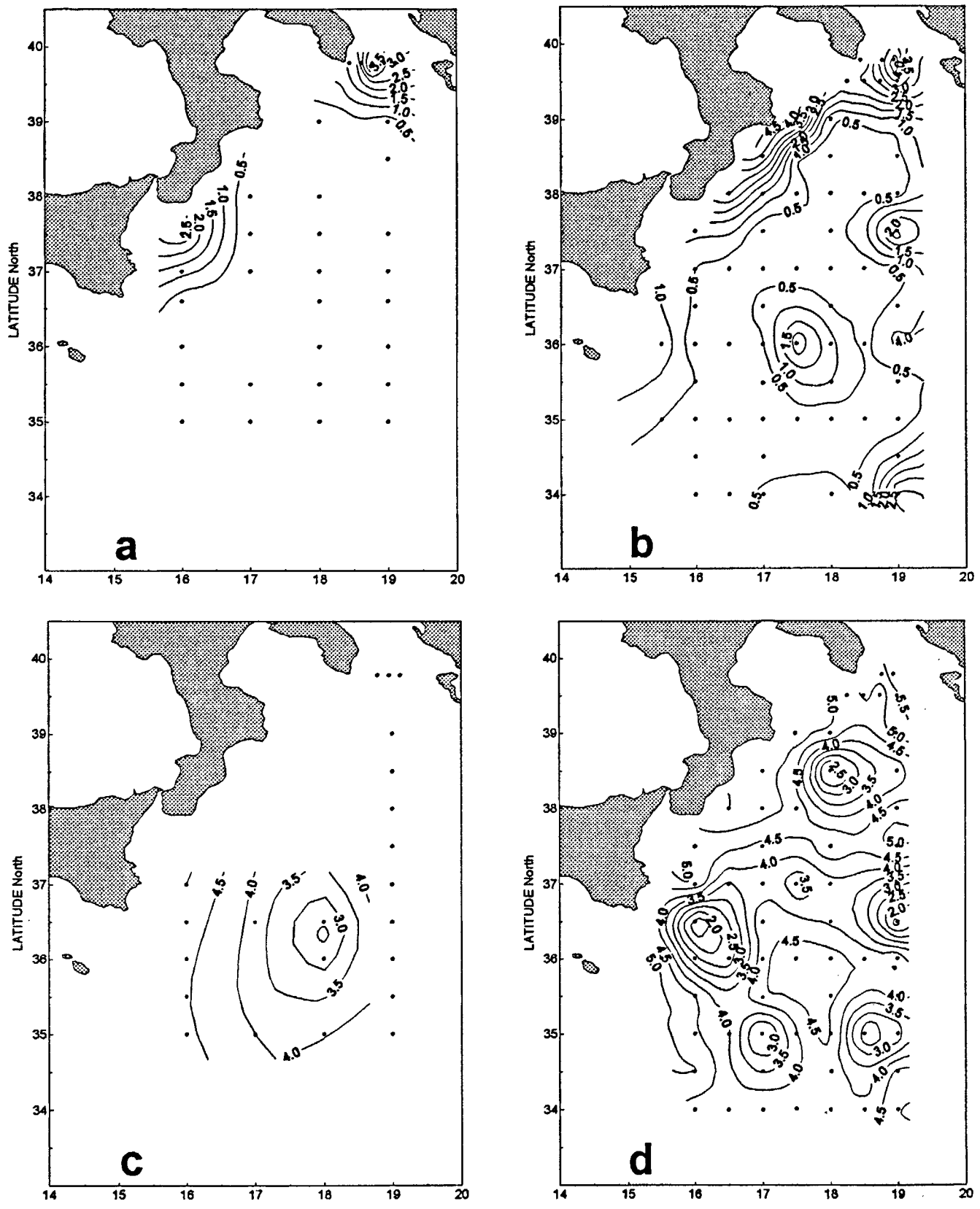

Figure 2

Horizontal distributions of nitrate (μM): a) POEM-BC-O91 at 100 m; b) POEM-BC-A92 at 100 m; c) POEM-BC-O91 at 300 m; d) POEM-BC-A92 at 300 m.

The GCM described above is coupled, after a spin-up of three years and nine months starting from January climatological data, with a nitrogen model giving the space and time evolution of nitrates, N, phytoplankton, P and detritus, D, all in nitrogen units.

The AEM equations are:

$$\frac{\partial N}{\partial t} = -(\vec{u} \bullet \nabla) N + K_H \nabla_h^2 N + K_V \frac{\partial^2 N}{\partial z^2} - FP + rD$$

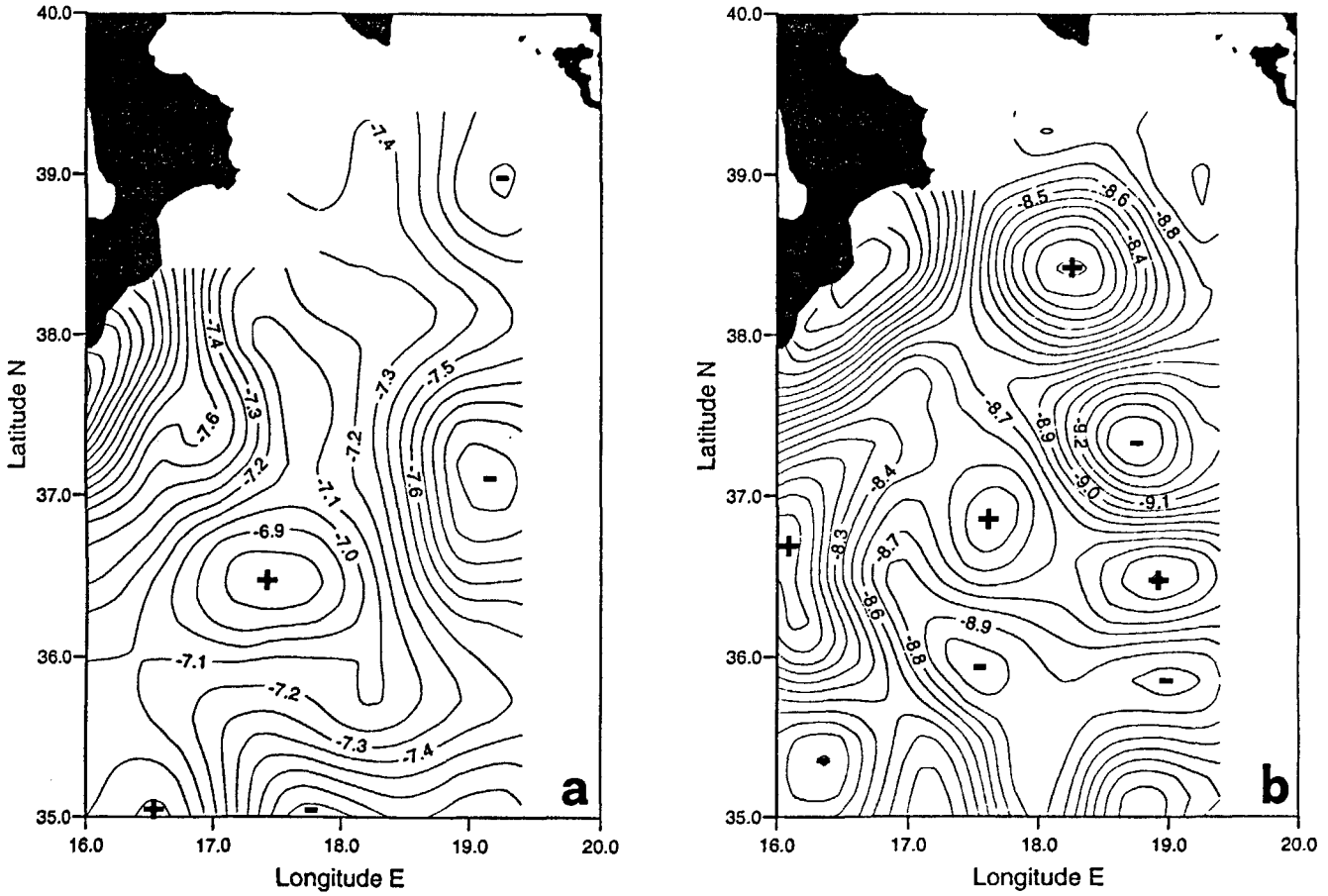

Figure 3

Geopotential anomaly at 20 dbar (R. Lev. 1200 dbar), courtesy P. Scarazzato: a) POEM-BC-O91; b) POEM-BC-A92.

$$\frac{\partial P}{\partial t} = -(\vec{u} \bullet \nabla) P + K_H \nabla_h^2 P + K_V \frac{\partial^2 P}{\partial z^2} + FP - dP$$

$$\frac{\partial D}{\partial t} = -(\vec{u} \bullet \nabla) D + K_H \nabla_h^2 D + K_V \frac{\partial^2 D}{\partial z^2} - rD + dP$$

where $\vec{u}$ is the computed total velocity and ∇_h^2 is the horizontal Laplacian.

The limiting factor F for the algal growth depends on the temperature T, given by the GCM, on the irradiance L_f and on the Michaelis-Menten uptake formulation, through the expression

$$F = g_{max}(T) L_f \frac{N}{C_N + N}$$

where C_N is the half-saturation constant for nitrogen.

The temperature limitation is computed using the Arrhenius' formulation (Eppley, 1972):

$$g_{max} = G_{max}\, e^{k_T T}$$

The formula for light limitation L_f is, following Steele (1962):

$$L_f = f \frac{\bar{I}}{I_{opt}} e^{1 - \frac{\bar{I}}{I_{opt}}}$$

The photoperiod f is given by the expression

$$f(day) = f_1 - f_2 \cos\left[\frac{2\pi(day + 10)}{365}\right]$$

where *day* is the julian day of the year.

The optimum light I_{opt} is chosen to be $I_0/2$ in accord with Steele (1962), where I_0 is the surface irradiance.

The non spectral formulation of the irradiance at depth z is given, according to UNESCO (1983), by the expression

$$\bar{I} = \frac{I_0(1 - e^{-k_z z})}{k_z z}$$

where k_z is the light extinction coefficient.

The equations for the biochemical tracers are active advection-diffusion equations solved at the same grid points of the hydrodynamics with no flux boundary conditions. The 16 vertical levels correspond to the same staggered grid of the hydrodynamics.

The nitrogen cycle is a dynamic balance of the three biological compartments and their sum, $\Sigma = N + P + D$, is conservative on a basin scale because every effect due to outer fluxes has been neglected: this means that, due to the horizontal exchanges, in a sub-basin the total nitrogen is generally not preserved.

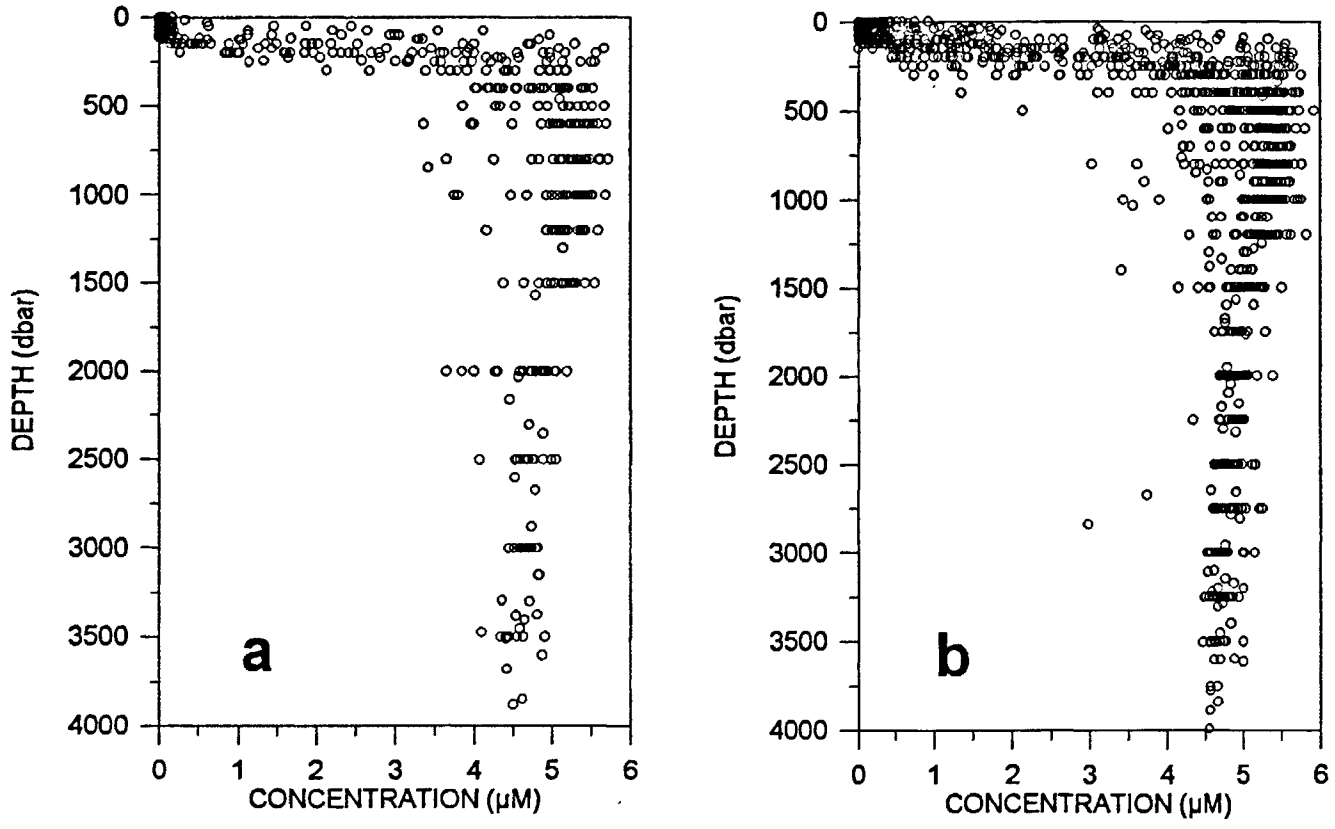

Figure 4

Cumulative plots of vertical distribution of nitrate: a) POEM-BC-O91; b) POEM-BC-A92.

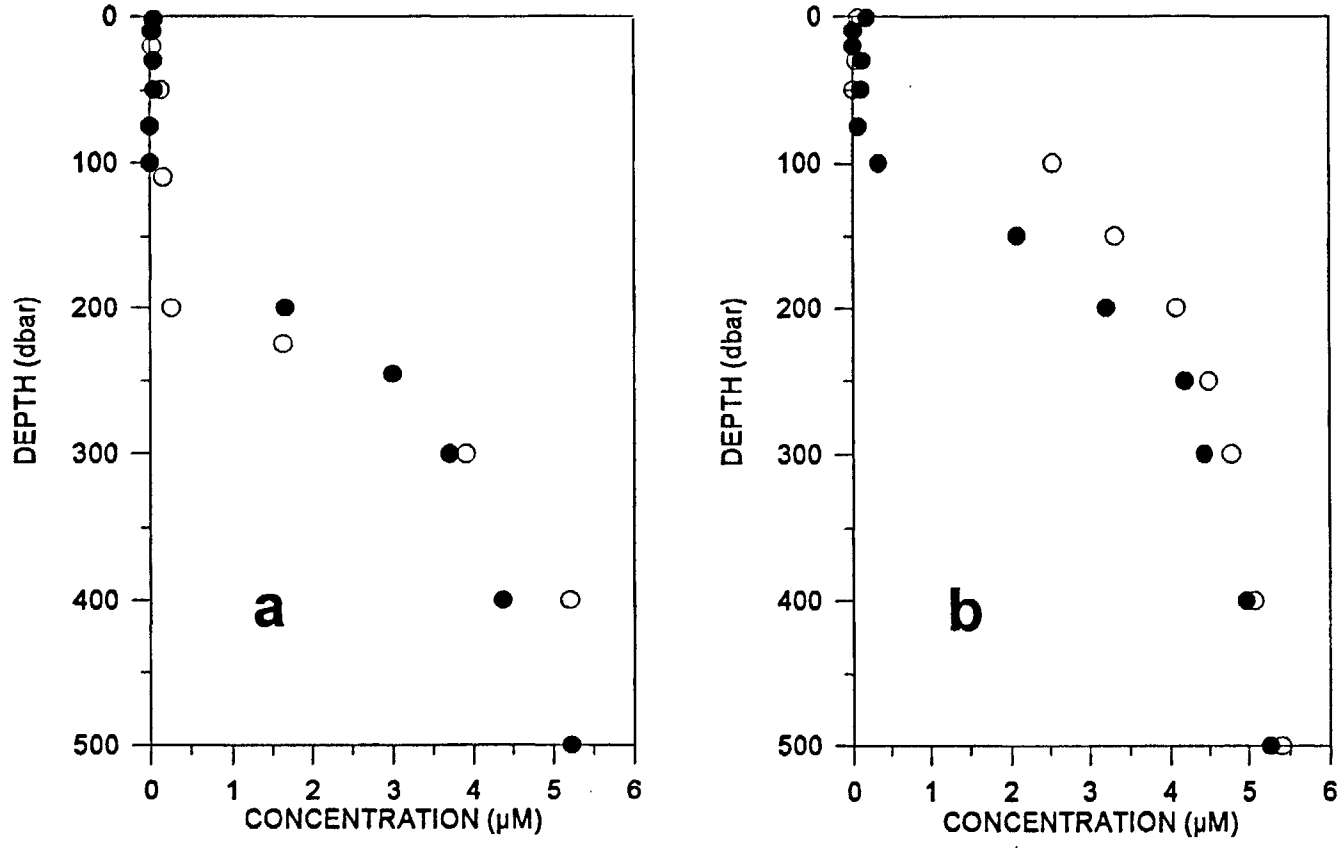

Figure 5

Vertical profiles of nitrate at the centre and the border of the gyres: a) POEM-BC-O91: ○ St. 308; ● St. 212. b) POEM-BC-A92: ○ St. 209; ● St. 211.

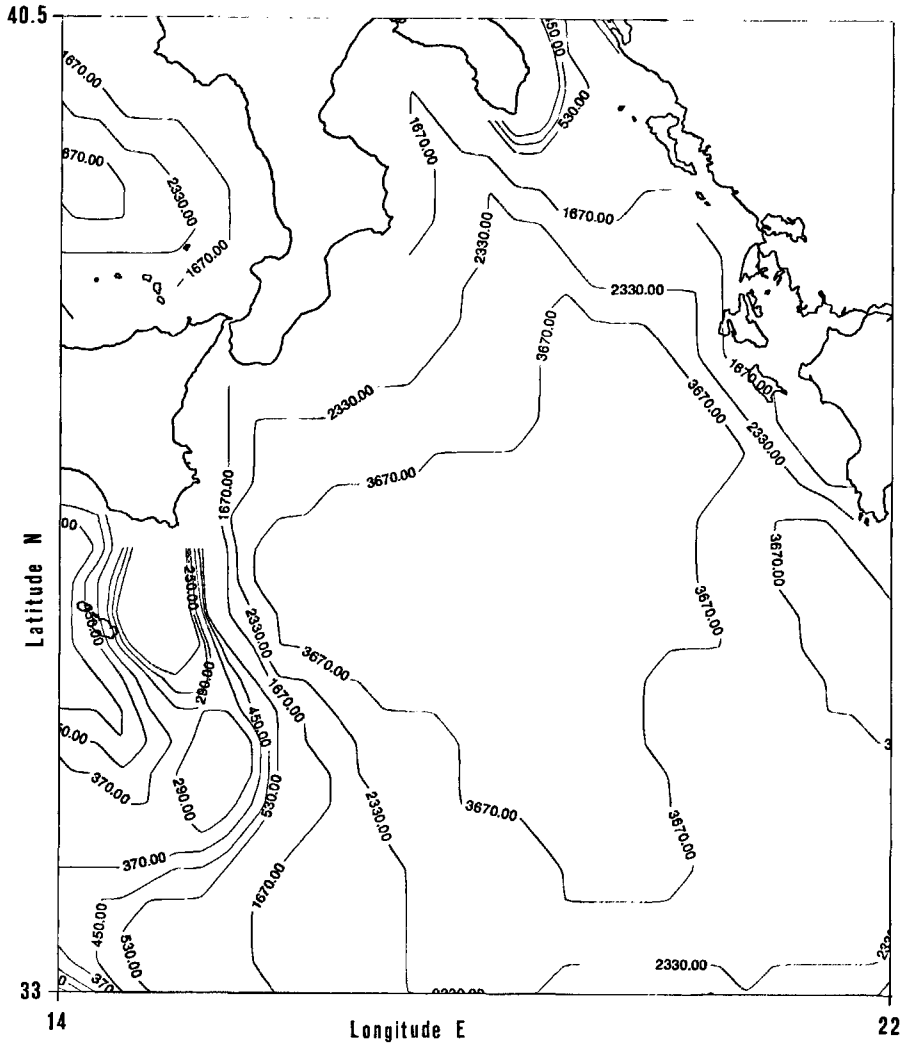

Figure 6

Ionian bottom depth in metres in the GCM.

In Table 1, the biological parameters used in this experiment are reported. The ranges proposed are presented in the quoted references and adapted to our model, using values typical of oligotrophic regions. In the case of the turbulence parametrization we resorted to an experimental calibration.

A simple scale analysis of the diffusion-transport equation can help us in evaluating the wind-driven advection *versus* the diffusion of the biological tracers.

With our K_H value and a current velocity of O (1 cm s^{-1}), a scale analysis gives the estimation of about 100 km as a typical detectable pattern length. This value is quite high in comparison with the spatial resolution of 1/4 degree (about 25 km). In fact, high eddy viscosity coefficients cause a strong damping of the mid-wavenumber processes, as demonstrated by Crise (1995).

We can compare the order of magnitude of the terms $K_H \nabla^2 \Sigma$ and $\vec{u} \cdot \nabla \Sigma$ in the advection-diffusion equation.

In one dimension

$$K_H \frac{\partial}{\partial x}\left(\frac{\partial \Sigma}{\partial x}\right) \cong O(10^7 10^{-7}) \frac{\partial \Sigma}{\partial x} = O(1) \frac{\partial \Sigma}{\partial x}$$

Table 1

Parameters used for the Ionian experiment.

Parameter	Definition	Unit	Value	Reference
C_N	nitrate half-saturation	μM	.2	(MacIsaac and Dugdale, 1969)
d	phytoplankton mortality	s^{-1}	5.55 10^{-7}	(Slagstad, 1982)
Gmax	maximum growth rate	s^{-1}	6.83 10^{-6}	(Eppley, 1972)
r	regeneration rate	s^{-1}	1.19 10^{-5}	(Slagstad, 1982)
k_T	temperature coefficient	$^{\circ}C^{-1}$	6.33 10^{-2}	(Eppley, 1972)
k_z	light attenuation	cm^{-1}	.006	(UNESCO, 1983)
I_{opt}/I_o	optimum light ratio		.5	(Steele, 1962)
f_1	photoperiod add. coef.		.5	(UNESCO, 1983)
f_2	photoperiod mul. coef.		.125	(UNESCO, 1983)
K_H	horizontal turbulent diffusion	$cm^2 s^{-1}$	8 10^6	(calibration)
K_V	vertical turbulent diffusion	$cm^2 s^{-1}$	1.5	(calibration)

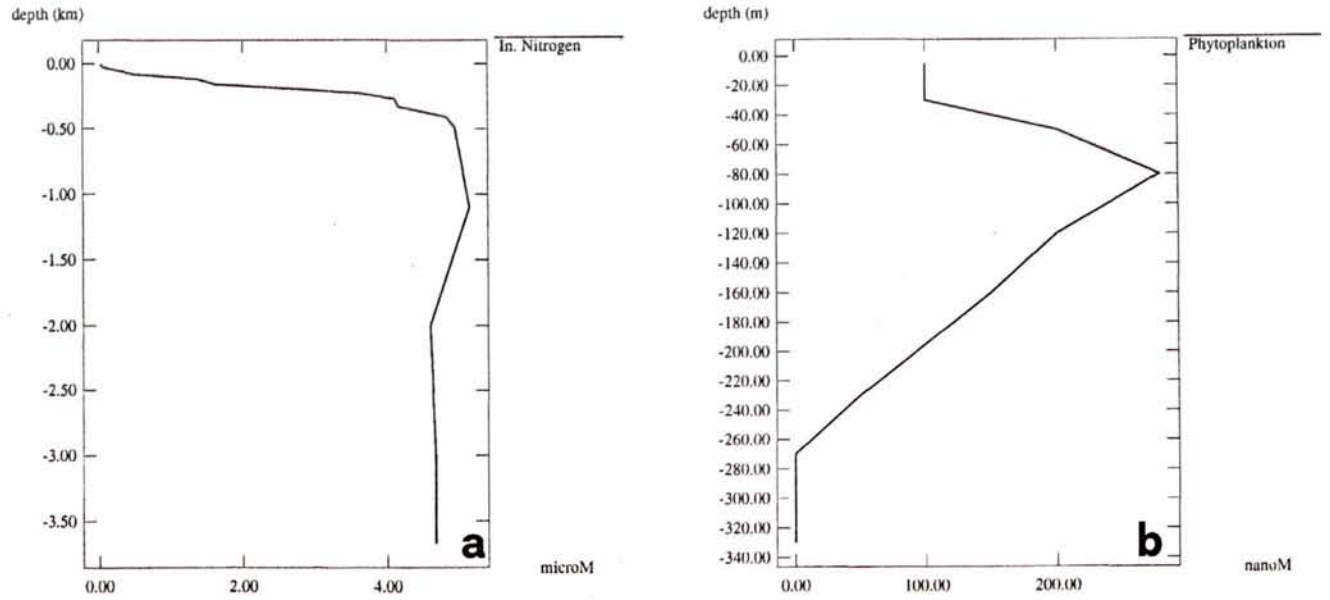

Figure 7

AEM initial profiles of: a) inorganic nitrogen; b) phytoplankton.

$$u\frac{\partial \sum}{\partial x} \cong O(1)\ \frac{\partial \sum}{\partial x}$$

if the typical scale for velocities is 1 cm s^{-1}.

So advection and diffusion have the same order of magnitude and are both in competition, at least when horizontal velocities are small. We can expect a diffusion-like tracer pattern when velocities are small and an advection-like pattern when velocities are high.

As first approximation we can safely assume, disregarding the other terms in the advection-diffusion equation, that if $\vec{u} \cdot \nabla \sum$ is 0, this implies that the tracer velocities are tangent to the tracer isolines (*i.e.* the streamlines exhibit the same behaviour as the tracer). On the other hand, if $\vec{u} \cdot \nabla \sum 0$ we can expect a diffusion-like pattern with the tracers isolines crossing the velocity vectors.

RESULTS

Seasonal effects on nitrogen distribution

The numerical experiment performed by the above-mentioned AEM is designed to investigate the seasonal variability influence on the nitrogen distribution.

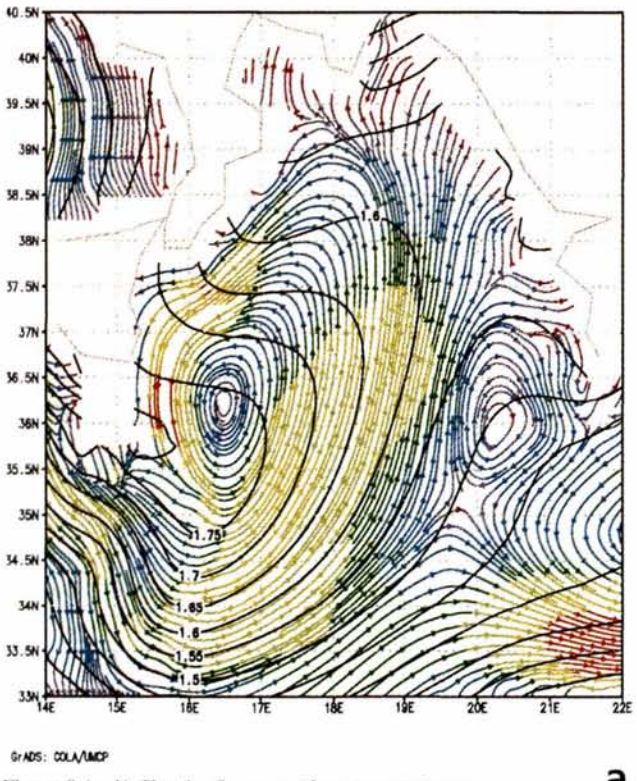

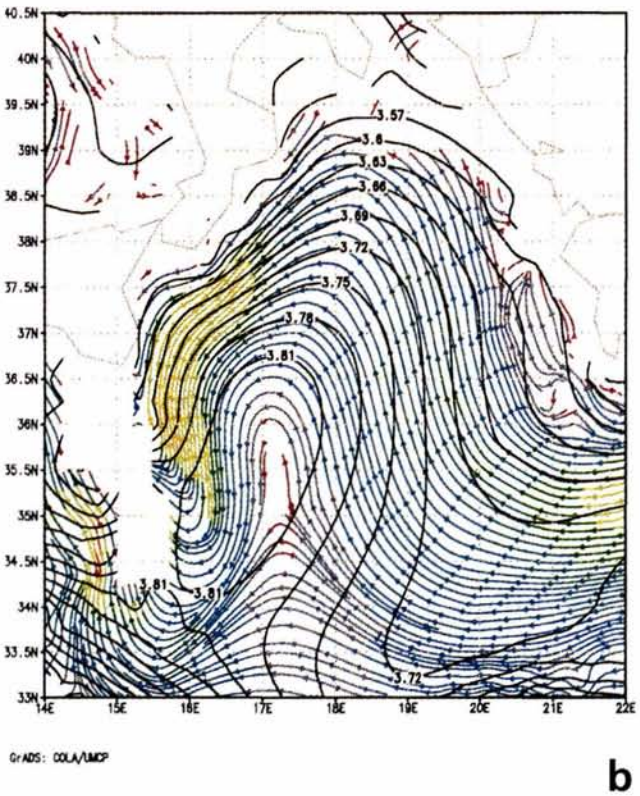

Figure 8 (*a, b*). For the figure captions see next page.

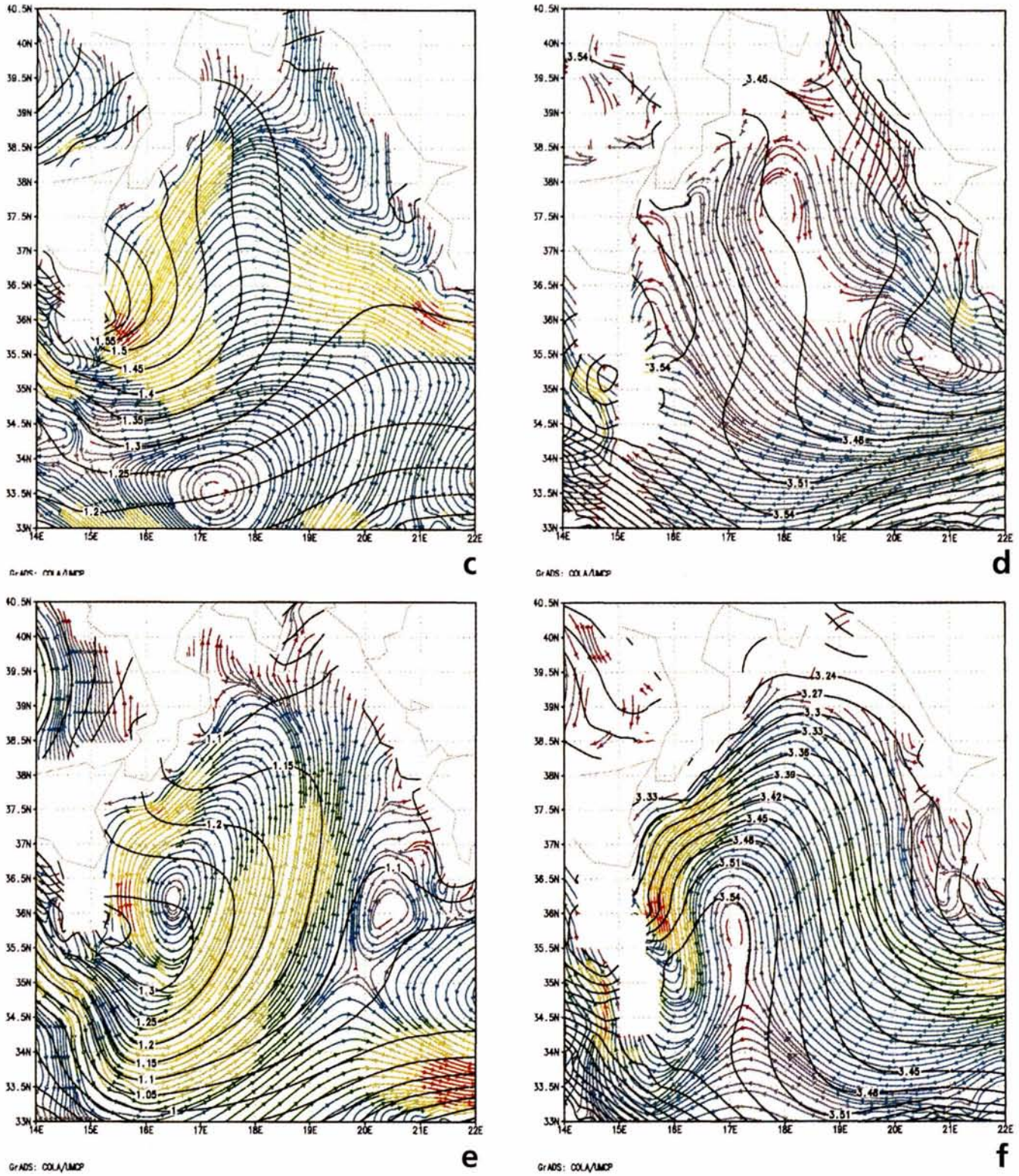

Figure 8 (*c, d, e, f*)

Monthly averaged horizontal distributions of total nitrogen (μM) in the Ionian Sea computed by the model (black isolines); streamlines of the nearer level are superimposed (red color - highest velocity, violet - about 0). The maximum velocity for each level is presented in parenthesis. a) ∑ at 80 m in April A1. (3 cm.s^{-1}). b) ∑ at 270 m in April A1. (2 cm.s^{-1}). c) ∑ at 80 m in October O1. (2 cm.s^{-1}). d) ∑ at 270 m in October O1. (1 cm.s^{-1}). e) ∑ at 80 m in April A2. (3 cm.s^{-1}). f) ∑ at 270 m in April A2. (2 cm.s^{-1}).

The ecological simulation begins after three years and nine months spin-up with the monthly mean October forcings. Thus we assume as initial conditions for inorganic nitrogen the vertical profile obtained as average of all NO_3 data collected during the cruise POEM-BC-O91. The phytoplankton vertical profile is derived from summer data after Berland *et al.* (1988). The initial detritus profile is chosen null everywhere. The initial vertical concentrations, reported in Figure 7, are identical throughout the basin.

In the following, we shall discuss the monthly mean field of total nitrogen obtained by the AEM on April, on October, and, as a comparison, on April again, respectively 6, 12 and 18 months after the AEM start-up, in correspondence with the POEM-BC-O91 and POEM-BC-A92 cruises. We shall call them A1, O1 and A2, respectively.

Let us analyse in greater detail the horizontal maps of total nitrogen at 80 and 270 depth: the choice of the first level is suggested by the practical absence of nutrients in the layer above 80 metres (Bregant *et al.*, 1992) and the second is in correspondence with the Levantine Intermediate Water (LIW) core (Nittis *et al., op.cit.*).

Let us evaluate the relative importance of upwelling and cyclonic circulation as source of inorganic nitrogen at 80 m depth in April (Fig. 8 *a*). An evident coastal signal is produced by the entrainment driven by coastal upwelling. This effect creates a nitrogen gradient because of the higher concentration of the nutrients entering the photic zone, which is depleted of organic and inorganic nitrogen. The other dynamic aspect is the westward intensification of the cyclonic circulation, generating an enhanced Σ transport which has an antagonistic effect with respect to diffusive term in the northern part of the Ionian cyclone: even within the maximum horizontal flow field area at 80 metres, we find that the Σ distribution is diffusion-driven in the northwestern Ionian circulation. In the southwestern region, however, the advection is stronger.

The Σ distribution at 270 m depth is different (Fig. 8 *b*): the LIW coming from the eastern basin is trapped in the gyre, showing a similar intensification on the western boundary, but the Σ isolines exibit an advective behaviour. This is influenced by the decreasing of the gradient of Σ (one order of magnitude less than that in Figure 8 *a*). The coastal upwelling has no direct effect on nutrient transport because of the small Σ vertical gradient and the reduced influence of the Ekman suction at this depth.

This effect is present beyond the euphotic zone, and suggests that the new production in April is essentially due to coastal upwellings and that the contributions from MAW and from the cyclonic circulation are relatively less important.

The topography influences the position of the centre of the vortex, which is almost coincident with the Σ maximum which forms a homogeneous spot of relatively high Σ concentration. To understand this effect, we can follow the discussion of a two-dimensional advection-diffusion problem of a concentration of a passive scalar in a vortex given by Young (1983). First of all we calculate the adimensional number $\mu = R^2\Omega/A_H$ where R is the radius of the vortex, and Ω the angular speed.

Assuming $R = O(100$ km$)$; $\Omega = O(10^{-7}$ s$^{-1})$; $K_H = O(10^7$ cm^2 s$^{-1})$, we obtain that $\mu = O(10)$.

In this computation the ratio between advection and diffusion in an eddy is 10. In the case of the strongest velocity, the so-called "weakly diffusive limit" predicts a homogenization of the tracer inside the eddy (Young and Rhines, 1982).

A substantially different scenario is depicted in Figures 8 *c* and 8 *d* and showing the October results. At 80 m depth, the typical summer situation of MAW inflow into the centre of the Ionian partially reverses the circulation, allowing the total nitrogen to diffuse in the same direction and pattern of the mean flow; nevertheless the streamlines cross the Σ isolines, exhibiting a diffusive pattern in the northern part of the Ionian gyre. The net effect is that a larger zone seems to be affected by the coastal upwelling in October than in April, when the effect of the upper circulation compresses the upcoming nutrients southward. The presence of other small-scale features such as the eddies in the southern part of the Ionian does not affect the distribution of Σ. At 270 m depth, the wind-driven circulation seems to be weakly anticyclonic. An almost homogeneous Σ field replenishes the Ionian basin with well-marked signature of the LIW in the southern part of the Ionian. A striking difference is present in the average values in our two reference levels: the upper layer shows a higher concentration of Σ in spring than in late summer, whereas the seasonal variation of circulation beyond 100 m reflects the anticyclonic regime modulation.

As a comparison, we show the A2 situation: the patterns present in A1 are still evident, and a cyclonic circulation is present again (Fig. 8 *e*, 8 *f*). The average values of Σ are higher in Figure 8 *e* than in Figure 8 *a* and the opposite for the deeper level (Fig. 8 *f vs* Fig. 8 *b*) because of the poor vertical balance of the model, but the gradients are similar. This fact can support our confidence in using the model as a tool for the investigation of differential time-integrated quantities such as annual fluxes and primary production.

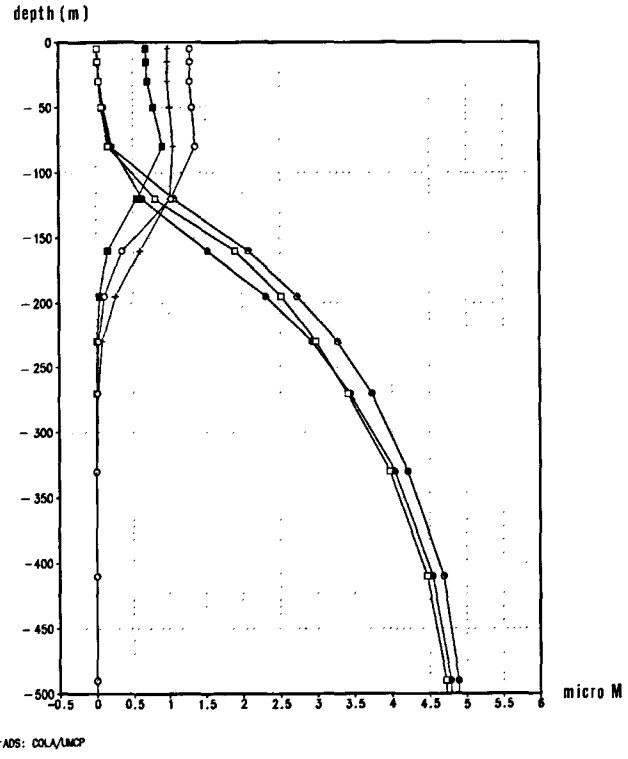

Figure 9

Monthly averaged vertical profiles of inorganic nitrogen and phytoplankton concentrations (all in μM) at 36 N 19 E: ○ inorganic nitrogen profile A1; ● inorganic nitrogen profile O1; □ inorganic nitrogen profile A2; ■ phytoplankton profile A1; + phytoplankton profile O1; ○ phytoplankton profile A2.

Vertical structure

Figure 9 shows the vertical structure for both phytoplankton and nutrient in the Ionian.

Surface layers are nutrient-depleted while phytoplankton is high. On the other hand, we have an increase in nutrients through the depth. A typical inorganic nitrogen profile (36.5° N, 19° E) exhibits different variability along the water column: we plot A1, O1, and A2 profiles. There is no seasonal signal for NO_3 in the upper layer; the reversal of the circulation induced by weakening of the wind stress causes the deepening of the nutricline during October and a successive rising in A2. After 350 m, the direct effect of the circulation seasonal variation is not present and only a progressive increasing of inorganic nitrogen concentration is present.

The phytoplankton profile shows a subsurface maximum which is in correspondence with the deep chlorophyll maximum found by Rabitti *et al.* (*op. cit.*), lying over the nutricline and vertically adjusting in accordance with its seasonal variations. In summary, we have a situation where the dynamics of phytoplankton is higher in intermediate waters due to the balance between light intensity and nutrient availability. On the other hand, surface and deep levels do not present a sensible seasonal signal.

Nitrogen fluxes and primary production

The quantitative behaviour of the nitrogen dynamics and of the phytoplankton production can be analysed considering the exchanges between the Ionian basin and the adjacent basins. The control in time and space of the AEM facilitates an estimation of the fluxes in terms of total nitrogen among the main areas of the Mediterranean Sea.

In particular, for the Ionian basin, we obtain a yearly decrease in the integrated components of inorganic and organic nitrogen. This value is 23.8 10^3 tons per year, equal to .03 % loss of the total nitrogen content of the Ionian Sea. Comparing this estimate with the loss of 354.2 10^3 tons per year of the Levantine basin plus the Aegean Sea, we see a striking difference, which is due essentially to the strong thermohaline interactions which are responsible for the convective mixing and the formation of the LIW. The net loss in inorganic nitrogen of the Ionian basin can be balanced from other sources in the form of remineralization of the dissolved organic nitrogen, river runoff, nitrogen fixation, and atmospheric and benthic exchanges.

The nitrogen estimated flux of the Adriatic Sea gives a contribution to the Ionian basin equal to 2.8 10^3 tons per year, which is of the same order of value as the 1.7 10^3 tons per year given by Zore-Armanda and Petkovic (1976) on the basis of experimental data. This result suggests that

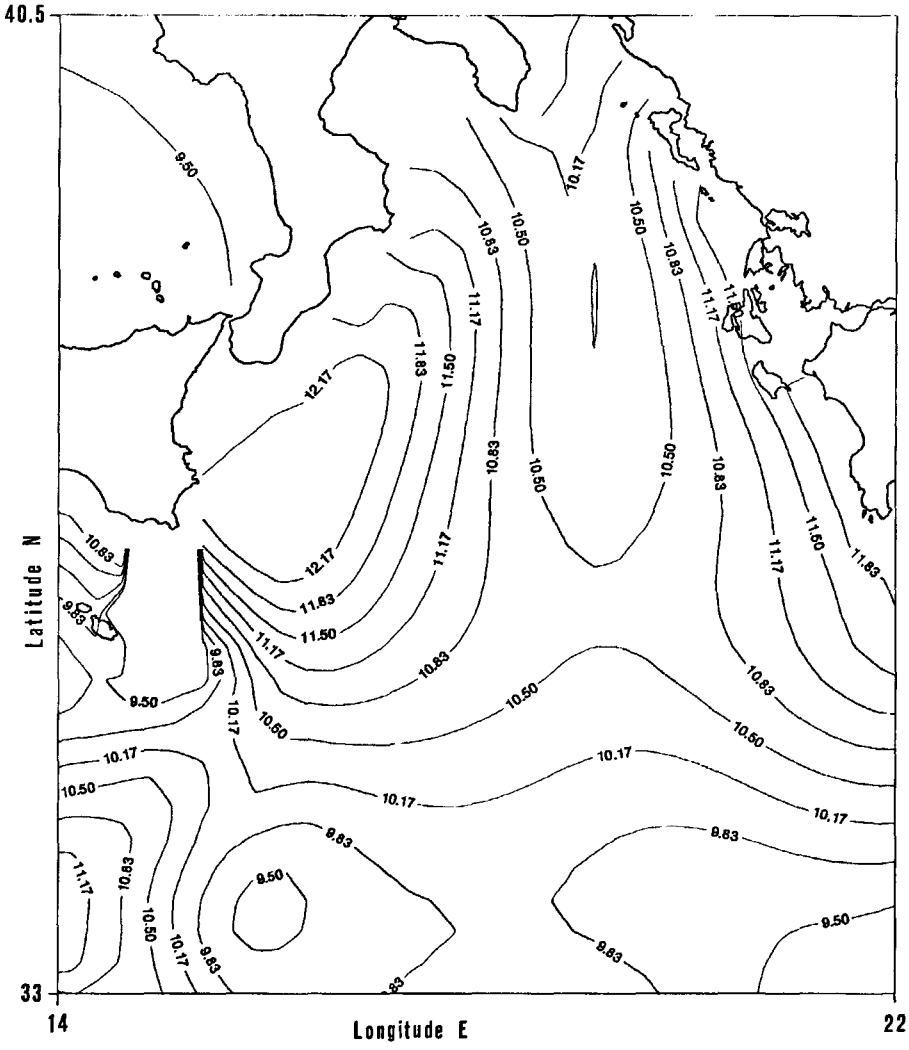

Figure 10

Vertically integrated annual primary production in the Ionian in gC m^{-2} yr^{-1}.

the Adriatic acts almost as a closed system, where the total exchanges with the Ionian are of minor importance.

The AEM dynamically evaluates total primary production as the temporal integral of the time rate of change of phytoplankton concentration. The map of the yearly, vertically-integrated primary production in the Ionian is given in Figure 10. It reaches its maximum value in correspondence with the upwelling area influenced by the cyclonic gyre present during spring, while the relative minimum in the southern Ionian Sea appears because of a persistent wide anticyclonic area.

The basin-averaged total primary production is 11.5 $gC\ m^{-2}\ yr^{-1}$. We rely throughout this paper on the carbon-nitrogen ratio proposed by Redfield *et al.* (1963), which is valid for oceanic ecosystems; but in some oligotrophic areas of the Eastern Mediterranean this ratio can be even higher by a factor of two (Dugdale and Wilkerson, 1988).

The primary production of the Ionian Sea is partly due to the entrainment of the nutrient because of upwelling and vertical mixing and the influence of MAW, and partly determined by the recycling of the nitrogen among the three compartments. The evaluation of the total nitrogen from the aphotic into the euphotic zone gives a contribution equal to 534.8 10^3 tons. This value also takes into account the organic nitrogen inflow at the Sicily Strait (81.1 10^3 tons), and on this basis the mean new production in the Ionian Sea can be estimated as 4.7 $gC\ m^{-2}\ yr^{-1}$. Moreover, the ratio of the new primary production versus total production, defined as the f-ratio by Eppley and Peterson (1979), is 0.4 in the Ionian Sea, with a recycling index of 2.5.

DISCUSSION

Within the model domain the advection/diffusion mechanisms ensure zones of high concentration of nutrients and phytoplankton despite horizontally homogeneous initial conditions.

This can be seen in the model results (Fig. 8) and is confirmed by the data interpretation (Fig. 2), even though a less energetic dynamics is shown by climatological model results: the tentative conclusion to be drawn is that heat fluxes intensify the general circulation structures and play a crucial role in the smaller scale transient features.

In October at 100 m depth, only a coastal upwelling area is present in the data (Fig. 2 *a*) and the lack of influence of the upper layer circulation in this case is confirmed by model results: no direct effect of the sub-basin circulation is evident and only the coastal upwelling is relevant for the total nitrogen distribution.

The meridional orientation of isolines near the Calabrian coast and the zonal distribution near the Maltese escarpment are well represented in the data, suggesting that the hydrodynamic considerations made for the model can also be applied to the data.

A southward shift of the upwelling area in the model can be related to the coarse resolution of the wind forcing.

At 300 m depth, the anticyclonic circulation of the basin causes a well defined minimum in the data in the centre of the Ionian (Fig. 2 *c*); this is also present in the Figure 8 *d*, but because of the effect of the strong diffusion, the nitrogen concentration gradient is smaller in modulus and the influenced area is wider.

In April, the data (Figs. 2 *b*, 2 *d*) present the signature of the cyclonic gyre in the centre of the basin at both 100 m and 300 m depth. At 300 m depth, smaller but energetic anticyclonic transient eddies surround the main structure. The simulated current is basically wind-driven and under this forcing the model is able to reproduce only the large scale cyclonic circulation giving a complete reversal of the flow field (Fig. 8 *a*, 8 *b*).

All the other anticyclonic eddies can probably be reproduced by a more appropriate thermohaline forcing. The model connects the Maltese upwelling with the circulation-induced entrainment, while the data show a clear separation of the coastal and offshore processes.

The vertical structure in the model is determined essentially by the internal dynamics of the nitrogen cycle, basically influenced by light and nutrient availability, as found also by Kiefer and Kremer (1981).

Comparison of this simplified vertical dynamics with some profiles exhibits the same gross structure for the nitrates (Fig. 5) and the inorganic nitrogen (Fig. 9): very low concentration in the euphotic zone in both periods, a seasonal variation of the nitracline due to physical and biological reasons, and a reduced dynamics in the lower nitracline part. Again, the seasonal variations are much less pronounced in the simulation than in the measured profiles, but the different seasonal regimes obtained by the model are in good agreement with the experimental profiles (the black-dot profiles in Figure 5 are to be compared with the profiles in Figure 9). A direct comparison in the centre of the gyres is difficult to achieve because of the different geographical position and the smaller seasonal signal in the model.

As regards phytoplankton, the model predicts high values due to the absence of grazing and sinking processes; a subsurface maximum is present in A1 and A2 profiles, but the poor vertical dynamics prevents quantitative reproduction of the vertical structure of the phytoplankton.

Nevertheless, some information on differential quantities, such as primary production, can be derived because the primary production is an estimation of the integral of the time rate of change in phytoplankton concentration and this estimate is only in the variation of the concentration.

Our estimation of the total primary production can be compared with the potential fertility figure of 6 $gC\ m^{-2}\ yr^{-1}$ after Béthoux (1981). This value takes into account the biological assimilation of the available nutrient in the entire Eastern Mediterranean Sea. Another estimation by Béthoux (1989), using the oxygen consumption throughout the Eastern Mediterranean after evaluation of vertical advection, gives 12 $gC\ m^{-2}\ yr^{-1}$. Thus the average of the total primary production calculated by the AEM is in good agreement with the above-mentioned estimated values, in particular with the second one, which also takes into account the vertical fluxes.

There are no experimental measures of the f-ratio in the Ionian Sea, instead, estimates were performed in other parts of the Mediterranean using different methods. Dugdale and Hopkins (1978) obtained an f-ratio of 0.3 in the Petalion Gulf of the Aegean Sea; Minas *et al.* (1988) estimated an f-ratio of 0.23 at the Cousteau floating laboratory in the Ligurian Sea; and Minas and Bonin (1988), on the Nice-Calvi section in the North Western Mediterranean, evaluated an f-ratio of 0.36. Thus our value of the f-ratio for the Ionian Sea is slightly higher than measures in other areas of the Eastern Mediterranean, and quite within the estimates made in the Western Mediterranean.

CONCLUSION

The description of biogeochemical processes by means of the hydrodynamical ecomodel permits the reproduction of some key aspects of the seasonal dynamics of the nitrogen cycle. Moreover this approach allows a first but significant verification of the ecomodel in comparison with observational data sets.

Model results and observational data suggest the importance of sub-basin features on tracer distribution. The euphotic layer circulation is strongly affected by the wind-stress curl and the response of the model is in good agreement with the observations. Only at the bottom of this layer do we observe a significant seasonal modulation of the cyclonic area present at the centre of the basin. Below, the thermohaline forcing is stronger and the model is unable to reproduce all the features present in the data even though it is able to capture the basic aspects of the nutrient distribution. In particular, areas of stronger circulation tend to transport the tracers in a passive-like manner, while areas of weak currents are subjected to tracer diffusion.

The vertical structure of the model requires refinement, including a better parameterization of the vertical diffusion and vertical mixing processes. Light greatly affects algal growth and a more sophisticated modelling of irradiance and cloudiness will improve the seasonal dynamics.

The lack of data on the Ionian Sea does not allow us to state, as Coste *et al.* (1988) have done for Gibraltar Strait, that the MAW inflow through the Sicily Strait is a source of additional new nitrogen, even if particulate organic carbon measurements and surface nutrient concentration data recently collected in the Sicily Strait and Ionian Sea (Rabitti *et al.*, 1994 *b*) seem to support the above considerations.

Even if the nutrient dynamics of the Ionian Sea is far from being fully understood due to the lack of extended chemical and biological observations, the above considerations suggest that the characteristics of the "marine desert" should be reassessed on the basis of a more complete biochemical approach.

Acknowledgments

This work was partially funded by the EC contract MAS2-CT93-0055.

The authors wish to thank Nadia Pinardi for her friendly encouragement and for the hydrodynamic model supply and Job Baretta and Bruno Manca for helpful discussions.

The OGS authors are indebted to Valentina Mosetti, who managed all the computer systems needed for this work. The authors are also indebted to Davide Bregant and Anna Luchetta for their support.

We dedicate this work to the memory of Antonio Michelato, chief scientist of the POEM-BC-A92.

REFERENCES

Berland B.R., A.G. Benzhitski, Z.P. Burlakova, L.V. Georgieva, M.A. Izmestieva, V.I. Kholodov, S.Y. Maestrini (1988). Conditions hydrologiques estivales en Méditerranée, répartition du phytoplancton et de la matière organique, *Oceanologica Acta* Special issue, **9**, 163-177.

Béthoux J.P. (1981). Le phosphore et l'azote en mer Méditerranée, bilans et fertilité potentielle, *Mar. Chem.* **10**, 141-158.

Béthoux J.P. (1989). Oxygen consumption, new production, vertical advection and environmental evolution in the Mediterranean Sea, *Deep-Sea Research* **36**, 5, 769-781.

Bregant D., G. Civitarese, A. Luchetta (1992). Chemical parameters distribution in the Ionian Sea during POEM-06 Cruise (October 1991), *Rapp. Comm. int. Mer Médit.* **33**, 395.

Bryan K. (1969). A numerical method for the study of the circulation of the world ocean, *J. Comput. Phys.* **4**, 347-376.

Cox M.D. (1984). A primitive equation three dimensional model of the ocean, GFDL Ocean Group Tech. Rep., 1, GFDL/NOAA, Princeton University.

Coste B., P. Le Corre, H.J. Minas (1988). Re-evaluation of the nutrient exchange in the Strait of Gibraltar, *Deep-Sea Res.* **35**, 767-775.

Crise A., G. Crispi, R. Mosetti (1992). Parallelization of a coupled hydrodynamical ecomodel, Tech. Rep. N.135, CNR/PFI.

Crise A. (1995). Diffusion in GCM: some considerations, Tech. Rep. No. 5/95-OGA-1.

Cruzado A. (1994). Chemistry of mediterranean water, in: *Western Mediterranean*, ed. by R. Margalef, Pergamon Press, 126-147.

Dugdale R.C., J.J. Goering (1967). Uptake of new and regenerated forms of nitrogen in primary productivity, *Limnol. Oceanogr.* **12**, 196-206.

Dugdale R.C., T.S. Hopkins (1978). Predicting the structure and dynamics of a pollution-driven marine ecosystem embedded in an oligotrophic sea, *Thalass. Jugosl.* **14**, 107-126.

Dugdale R.C., F.P. Wilkerson (1988). Nutrient sources and primary production in the Eastern Mediterranean, *Oceanologica Acta* Special issue, **9**, 179-184.

Eppley R.W. (1972). Temperature and phytoplankton growth in the sea, *Fish. Bull.* **70**, 1063-1085.

Eppley R.W., B.J. Peterson (1979). Particulate organic matter flux and planktonic new production in the deep ocean, *Nature* **282**, 677-680.

Golnaraghi M., A.R. Robinson (1994). Dynamical Studies of the Eastern Mediterranean Circulation, in: *Ocean Processes in Climate Dynamics: Global and Mediterranean Examples*, ed. by P. Malanotte-Rizzoli and A.R. Robinson, Kluwer, 395-406.

Kiefer D.A., J.N. Kremer (1981). Origins of vertical patterns of phytoplankton and nutrients in the temperate, open ocean: a stratigraphic hypothesis, *Deep-Sea Res.* **28A**, 10, 1087-1105.

Kovacevic V., B. Manca, A. Michelato, P. Scarazzato (1994). DATA REPORT Cruise POEM-BC-October 1991 - Ionian Basin and Sicily Strait Part I: Hydrological and CTD Data, Tech. Rep. No. 2/94-OGA-1.

MacIsaac J.J., R.C. Dugdale (1969). The kinetics of nitrate and ammonia uptake by natural populations of marine phytoplankton, *Deep-Sea Res.* **16**, 45-57.

Malanotte-Rizzoli P., A. Bergamasco (1991). The wind and thermally driven circulation of the Eastern Mediterranean Sea, Part II: the baroclinic case. *Dyn. Atm. Oceans* **15**, 355-419.

Margalef R. (1978). Life-forms of phytoplankton as survival alternatives in an unstable environment, *Oceanologica Acta* **1**, 4, 493-509.

Michelato A., V. Kovacevic, B. Manca, P. Scarazzato, D. Viezzoli (1992). Hydrography and circulation of the Ionian Sea (1988-1991), *Rapp. Comm. int. Mer Médit.* **33**, 223.

Minas H.J., M.-C. Bonin (1988). Oxygénation physique et biologique de la Méditerranée nord-occidentale en hiver et au printemps. *Oceanologica Acta* Special issue **9**, 123-132.

Minas H.J., M. Minas, B. Coste, J. Gostan, P. Nival, M.-C. Bonin (1988). Production de base et de recyclage; une revue de la problématique en Méditerranée nord-occidentale. *Oceanologica Acta* Special issue **9**, 155-162.

Nittis K., N. Pinardi, A. Lascaratos (1993). Characteristics of the Summer 1987 Flow Field in the Ionian Sea, *J. Geoph. Res.* **98**, C6, 10.171-10.184.

Pinardi N., A. Navarra (1993). Baroclinic wind adjustment processes in the Mediterranean Sea, *Deep-Sea Res.* **40**, 6, 1299-1326.

POEM Group (1992). General circulation of the Eastern Mediterranean, *Earth-Science Review* **32**, 285-309.

Rabitti S., F. Bianchi, A. Boldrin, L. Daros, G. Socal, C. Totti (1994 *a*). Particulate matter and phytoplankton in the Ionian Sea, *Oceanologica Acta* **17**, 3, 297-307.

Rabitti S., G. Civitarese, M. Ribera (1994 *b*). DATA REPORT Cruise POEM-BC-October 1991 - Ionian Basin and Sicily Channel Part II: Chemical and Biological Data, Tech. Rep. No. 13/94-CNR/IBM.

Redfield A.C., B.H. Ketchum, F.A. Richards (1963). The Influence of Sea Water, in: *The Sea*, Vol. 2, ed. by M.N. Hill, Interscience, New York, 26-77.

Roether W., R. Schlitzer (1991). Eastern Mediterranean deep water renewal on the basis of chlorofluoromethane and tritium data, *Dyn. Atmos. Oceans* **15**, 334-354.

Slagstad D. (1982). A model of phytoplankton growth-effects of vertical mixing and adaptation to light. Modeling, Identification and Control, **3**, 2, 111-130.

Steele J.H. (1962). Environmental control of photosynthesis in the sea, *Limnol. Oceanogr.* **7**, 137-150.

UNESCO (1983). Quantitative analysis and simulation of Mediterranean coastal ecosystem: the Gulf of Naples, a case study, UNESCO Reports in Marine Sciences, 20.

Young W.R. (1983). The role of the boundary layer in gyre-scale ocean mixing, *J. Phys. Oceanogr.* **14**, 478-483.

Young W.R., P.B. Rhynes (1982). A theory of the wind-driven circulation. II Gyres with western boundary layers. *J. Mar. Res.* **40**, 849-872.

Zore-Armanda M., T. Pucher-Petkovic (1976). Some dynamic and biologic characteristics of the Adriatic and other basins of the Eastern Mediterranean Sea, *Acta Adriatica* **18**, 17-28